Hydrogen-bonding Pathways affecting Chemical Reactivity of Mandelylasparagine and Related Compounds

Elena Gaggelli and Gianni Valensin *
Department of Chemistry, University of Siena, 53100 Siena, Italy
Giorgio Adembri, Angela M. Celli, Mirella Scotton, and Alessandro Sega
Institute of Organic Chemistry, University of Siena, 53100 Siena, Italy

The different behaviour of L-(+)-*N*-mandelyl-L-(−)-asparagine, *N*-mandelyl-2-amino-4-pentanoic acid and *N*-mandelyl-2-aminobutanoic acid towards acylation was considered. ^{13}C And ^{1}H n.m.r. non-selective and selective relaxation rates and ^{1}H-{^{1}H} n.O.e.s were taken to show that L-(+)-*N*-mandelyl-L-(−)-asparagine assumes, in DMSO solution, a conformation quite different from that of the other two amino acids. In this conformation both lone pairs of the alcoholic oxygen were shown to be involved in hydrogen bonding and to be shielded in a way that makes approach of the acylating reagent difficult.

One of us prepared[1] the *O*-acetyl derivatives of the two diastereoisomers of *N*-mandelyl-L-(−)-asparagine (**1a** and **b**) in an endeavour to explain a case of partial racemates. Attempts to acetylate compounds (**1a** and **b**) using acetyl chloride or acetic

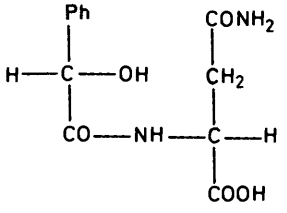

(1a)

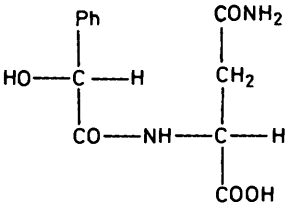

(1b)

anhydride under many different conditions were unsuccessful. To overcome the problem, L-(−)-asparagine was treated with *O*-acetylmandelyl chloride under controlled alkaline conditions. Though the synthetic goal had been reached, a wish to explain the failure of (**1a** and **1b**) to acetylate remained. This behaviour was odd when compared with numerous *N*-mandelylamino acids which could be easily acylated.[2]

The *N*-mandelylaspartic acids (**2**) exhibited the same behaviour as compounds (**1a** and **b**). It was thus supposed that the acylating agents could not react with the hydroxy group of the mandeloyl moiety because it was linked through a bifurcated hydrogen bond in which the $CONH_2$ or COOH group was involved.[2,3] The presence of $CONH_2$ or COOH was regarded as essential, as *N*-mandelyl-2-amino-4-oxopentanoic acid (**3**), for instance, could be easily acylated.

Because we would establish the molecular conformation in solution and in view of the close relationship between reactivity (especially biological activity) and conformation, we were led to re-examine the problem.

We dealt with the problem by n.m.r., taking advantage of conformation-sensitive parameters such as the ^{1}H–^{1}H intramolecular n.O.e. and spin–lattice relaxation rates. We studied L-(+)-*N*-mandelyl-L-(−)-asparagine (**1b**) and compared its spectral features with those of *N*-mandelyl-2-amimo-4-oxopentanoic acid (**3**) and *N*-mandelyl-2-aminobutanoic acid (**4**). The CH_2CONH_2 moiety in (**1b**) is substituted by CH_2COCH_3 and CH_2CH_3 in (**3**) and (**4**) respectively.

Due to the low solubility in water, dimethyl sulphoxide (DMSO) was chosen as the solvent for n.m.r. studies. In order to compare chemical reactivity and conformation features in solution, acylations were repeated using DMSO as solvent and the same difference in reactivity was found.

Table 1. ^{13}C N.m.r. chemical shifts for 0.2 mol dm^{-3} solutions in [$^{2}H_6$]DMSO

Carbon	(1)	(4)	(3)
CH_3		10.0	29.7
C(4)	36.4		44.0
C(3)	48.0	52.0	47.2
C(1)	73.2	72.4	73.0
C(2′)	127.0	125.1	126.7
C(4′)	127.4	126.2	127.2
C(3′)	127.8	126.8	127.7
C(1′)	141.1	139.8	140.9
C(2)	171.5	169.9	171.4
C(5)	171.7		
$CO(CH_3)$			213.2
C(6)	172.5	171.0	172.2

Table 2. ^{13}C Spin–lattice relaxation rates, R_1/s^{-1}, of protonated carbons for 0.2 mol dm^{-3} solutions in [$^{2}H_6$]DMSO

Carbon	(1)	(4)	(3)
C(4′)	3.45	2.54	2.77
C(2′)	1.60	1.08	1.21
C(3′)	1.61	1.12	1.24
C(1)	3.32	1.96	2.05
C(3)	4.59	2.18	2.12
C(4)	8.33	3.07	3.03
CH_3		0.75	0.50

Errors were evaluated in the range of ±4—7% confidence limits of the exponential regression analysis.

Results and Discussion

^{13}C-Spin–Lattice Relaxation Rates.—^{13}C Chemical shifts of the investigated compounds are reported in Table 1. The ^{13}C spin–lattice relaxation rates (R_1) of the three compounds are

Table 3. Correlation times τ_c,τ_G/ns for protonated carbons

Carbon	(1)	(4)	(3)
C(4′)	0.160	0.118	0.129
C(2′),C(3′)	0.030	0.021	0.022
C(1)	0.155	0.091	0.095
C(3)	0.213	0.101	0.098
C(4)	0.194	0.071	0.070
CH_3		0.012	0.008

Errors in correlation times were evaluated in the same range of errors in the measured ^{13}C spin–lattice relaxation rates

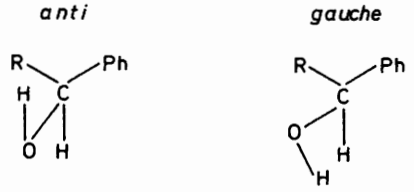

(1) R = CONHCH(COOH)CH_2CONH_2
(2) R = CONHCH(COOH)CH_2COOH
(3) R = CONHCH(COOH)CH_2COCH_3
(4) R = CONHCH(COOH)CH_2CH_3

Figure 1. *anti* and one of the possible *gauche* conformers of compounds (1)—(4)

reported in Table 2; the correlation times for protonated carbons are summarized in Table 3. For comparative purposes, numbering of all structures follows that shown in Figure 2.

It is known[4,5] that ^{13}C R_1 values are almost exclusively determined by dipolar interactions with directly bonded or nearby protons, thus allowing suitable delineation of the molecular dynamics. The motional features of aromatic carbons were first considered since they have fewer degrees of freedom if compared with side-chain carbons. The relaxation rate of the *para* carbon atom is in every case faster than those of the other aromatic carbons, suggesting that C(1′)–C(4′) is always the main rotation axis of the benzene ring. The relaxation rates of C(2′) and C(3′) are very similar such that an anisotropic model consisting of rotational reorientation around the main molecular axis with some degree of internal motions could be applied in every case[6] [equation (1) with $A = 0.25(3\cos^2\theta - 1)^2$, $B = 3(\sin^2\theta\cos^2\theta)$, and $C = 0.75(\sin^4\theta)$].

$$\frac{1}{nT_1} = \frac{\hbar^2\gamma_H{}^2\gamma_C{}^2}{r_{CH}{}^6}\tau_c\left\{A + B\frac{3\tau_G}{3\tau_G + \tau_c} + C\frac{6\tau_G}{6\tau_G + \tau_c}\right\} \quad (1)$$

In equation (1), τ_c is the main rotational correlation time, τ_G is the correlation time for librational motions of the aromatic ring, r_{CH} is the length of the C–H bond, n is the number of protons attached to the carbon under consideration, and θ is the angle between the main rotation axis and the C–H vector.

The main correlation time, τ_c, can be calculated by considering R_1 of C(4′): since the C–H vector lies on the main axis (in this case), equation (2) can be applied. This holds for a

$$\frac{1}{T_1} = \frac{\hbar^2\gamma_H{}^2\gamma_C{}^2}{r_{CH}{}^6}\tau_c \quad (2)$$

pure dipole–dipole relaxation mechanisms within the 'extreme narrowing' region.[7] As all protonated carbons exhibit maximum

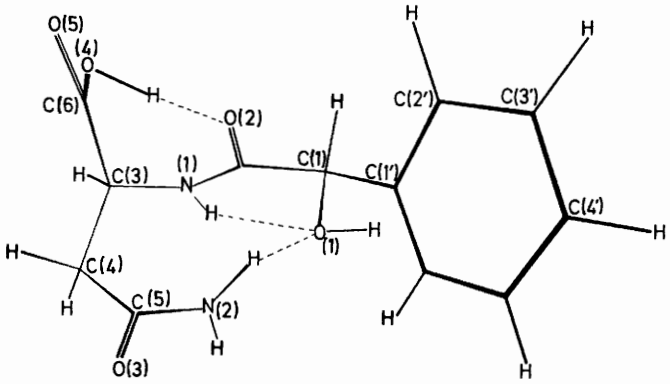

Figure 2. Projection of the Dreiding model of the 'most probable' conformation of compound (1) in [$^2H_6$]DMSO solution. Dashed lines are hydrogen bond pathways. The numbering system is that used throughout the text

^{13}C-{^1H} n.O.e.s, equation (2) was used to extract τ_c values and τ_G values were then obtained by applying equation (1). All correlation times are summarized in Table 3. Since the investigated molecules are quite flexible, the n.m.r. results must be interpreted as an effective weighted average among several instantaneous situations.

Consistent values of τ_c and τ_G are found for (3) and (4), suggesting very similar dynamics for the benzene rings in these compounds. In (1), on the other hand, both ring motions are governed by significantly greater correlation times yielding evidence of slowed motional dynamics for the aromatic moiety. This first conclusion is somewhat surprising if it is considered that the same molecular network is found in the near neighbourhood of the aromatic ring.

The correlation times of side-chain carbons, calculated by equation (2), ratify the conclusion that the molecular dynamics of (1) are quite different from those in both (3) and (4). In these last compounds increase in motional freedom can be noticed when going to side-chain carbons [correlation times as fast as 0.095 and 0.091 ns are calculated for C(1) in (3) and (4) respectively compared with 0.129 and 0.118 ns respectively for the main rotational motion]; the correlation times for C(3) (0.098 and 0.101 ns respectively) do not show any further increase in motional freedom, which is however achieved by the methylene groups (0.070 and 0.071 ns are the respective correlation times). The fact that terminal methyls have slower relaxation rates than those of methylenes is a direct proof of segmental motion.[4] It is therefore evident that (3) and (4) display common dynamic features in solution, thus suggesting that the two compounds are very likely to assume average conformations very similar to each other.

All correlation times of protonated carbons of (1), if compared with those in (3) or (4), are somewhat longer and are therefore consistent with the slowing down of motional dynamics. The main rotational correlation time of the benzene ring is so close to that of C(1) (0.160 and 0.155 ns respectively) that it might be appropriate to consider C(4′)–C(1) as the main rotational axis. Furthermore, on going to C(3), the correlation time is consistent with loss of motional freedom in striking contrast with the situation in both (3) and (4). Finally the correlation time of methylene carbon (0.194 ns) is very close to that of C(3) (0.213 ns), thus excluding the occurrence of segmental motion.

The great difference in dynamic behaviour in solution between (1) and (3) or (4) is a surprising event if the closeness of the chemical structures of the three compounds is considered, especially for (1) and (3) where the only difference is a methyl in place of an amino group. We therefore conclude that the

Table 4. ^{1}H N.m.r. parameters for 0.2 mol dm^{-3} solutions in [$^2H_6$]DMSO

	δ (p.p.m.)				*J*/Hz		
Proton	(1)	(4)	(3)		(1)	(4)	(3)
CH_3		0.76 (t)[a]	2.07 (s)[b]	$^3JCH_3$,C(4)H		7.4	
C(4)H[d]	2.54 (dd)[c]	1.72 (m)[e]	2.93 (d)[f]	$^3JC(4)H,C(3)H$	5.2		5.6
	2.68 (dd)						
C(3)H	4.50 (m)	4.18 (m)	4.53 (m)	$^2JC(4)H,C(4)H$	15.5		
C(1)H	4.90 (d)	4.97 (s)	4.90 (s)				
O(1)H	6.30 (d)	6.32 (p)[g]	6.27 (p)	$^3JC(1)H,O(1)H$	4.8		
N(2)H	6.93 (p)						
ArH	7.18—7.51 (m)	7.22—7.45 (m)	7.24—7.41 (m)	$^3JC(3)H,N(1)H$	9.0	7.9	8.4
N(1)H	8.18 (d)	7.93 (d)	8.17 (d)				
O(4)H	12.57 (b)[h]	12.74 (b)	12.89 (b)				

[a] Triplet. [b] Singlet. [c] Double doublet. [d] Shifts of the two protons could be inverted. [e] Multiplet. [f] Doublet. [g] Peak. [h] Broad peak.

Table 5. Mono-selective (R_i^s) and doubly selective (R_{in}^{ds}) spin–lattice relaxation rates (s^{-1}) for selected protons of 0.2 mol dm^{-3} (**1**), (**3**), and (**4**) in [$^2H_6$]DMSO

Relaxation rate	(1)	(4)	(3)
R^s[C(1)H]	1.29	1.16	1.18
R^{ds}[C(1)H,O(1)H]	1.51	1.21	1.22
R^s[N(1)H]	5.03	2.80	
R^{ds}[N(1)H,C(3)H]	5.05	3.06	
R^s[O(1)H]	25.77	19.68	18.52

Errors were evaluated in the range ±2—5% confidence limits of the exponential regression analysis.

Table 6. Selected proton–proton intramolecular distances (Å) for (**1**) and (**4**)

Proton pair	(1)	(4)
C(1)H–O(1)H	2.44	2.79
C(1)H–N(1)H	2.70	2.69
C(3)H–N(1)H	2.62	2.24
O(1)H–N(1)H	2.98	
N(2)H–C(1)H	2.85	
N(2)H–C(3)H	3.74	

Because of the dependence upon $1/r^6$, large errors (±5%) in proton spin–lattice relaxation rates and in motional correlation times yield relatively small errors (±2—4%) in the distances.

significant change in dynamic features very likely arises from some relevant change in the preferred average conformation.

^{1}H-*Selective Spin–Lattice Relaxation Rates.*—^{1}H Chemical shifts and coupling constants are summarized in Table 4. Monoselective (R_i^s) and doubly selective (R_{in}^{ds}) spin–lattice relaxation rates of some protons of 1, 3, and 4 are reported in Table 5.

The measurement of ^{1}H non-selective (R_i^{ns}), monoselective (R_i^s), and doubly selective (R_{in}^{ds}) spin–lattice relaxation rates has been suggested as a suitable aid to conformational studies in solution.[8–10] In the limit of 100% contribution from the ^{1}H–^{1}H dipole–dipole relaxation mechanisms expressions (3)—(5) can

$$R_i^{ns} = \sum_{i \neq j} \rho_{ij} + \sum_{i \neq j} \sigma_{ij} \quad (3)$$

$$R_i^{s} = \sum_{i \neq j} \rho_{ij} \quad (4)$$

$$R_{in}^{ds} = \sum_{i \neq j} \rho_{ij} + \sigma_{in} \quad (5)$$

be given[8–10] where ρ_{ij} and σ_{ij} are the direct- and cross-relaxation rates respectively for any proton pair [equations (6) and (7)][11] where r_{ij} is the interproton distance, ω is the proton

$$\rho_{ij} = \frac{1}{10}\frac{\hbar^2\gamma_H^4}{r_{ij}^6}\left\{\frac{3\tau_c}{1+(\omega\tau_c)^2} + \frac{6\tau_c}{1+(2\omega\tau_c)^2} + \tau_c\right\} \quad (6)$$

$$\sigma_{ij} = \frac{1}{10}\frac{\hbar^2\gamma_H^4}{r_{ij}^6}\left\{\frac{6\tau_c}{1+(2\omega\tau_c)^2} - \tau_c\right\} \quad (7)$$

Larmor frequency, and τ_c is the motional correlation time. It is evident from equations (4) and (5) that equation (8) holds which,

$$R_{in}^{ds} - R_i^s = \sigma_{in} = \frac{1}{10}\frac{\hbar^2\gamma_H^4}{r_{in}^6}\left\{\frac{6\tau_c}{1+(2\omega\tau_c)^2} - \tau_c\right\} \quad (8)$$

in the limit of extreme narrowing region, reduces to (9). Then

$$\sigma_{in} = \frac{1}{2}\frac{\hbar^2\gamma_H^4}{r_{in}^6}\tau_c \quad (9)$$

measuring doubly selective and monoselective proton spin–lattice relaxation rates allows determination of proton–proton distances if τ_c is known from other sources.

The [C(1)H–O(1)H] was calculated by measuring R[C(1)H–O(1)H]^{ds} and R[C(1)H]^s for the three compounds; then the three C(1)H–O(1)H distances could be calculated by using the correlation time from ^{13}C relaxation data in equation (9) (Table 6). The calculated distances correspond to a *gauche* conformer in the case of (**1**) (2.44 Å) and to an *anti* or nearly *anti* conformer in the case of (**4**) (2.79 Å) and (**3**) (2.88 Å) (see Figure 1).

Distances calculated from selective proton spin–lattice relaxation rates are more accurate than those calculated from homonuclear Overhauser enhancements and thus the C(1)H–O(1)H distances have a key role in quantitative analysis of n.O.e.s. Every calculated distance must, of course, be considered as a weighted average among several possible geometries in solution.

Moreover, proton relaxation rates can also be used for qualitative inferences. It is worth noting that the monoselective relaxation rates of the hydroxylic proton are close to each other in (**3**) and (**4**) whereas that in (**1**) is quite faster. Inspection of equation (4) suggests that a faster selective relaxation rate could be due either to a longer correlation time or to a larger number of proton–proton pairwise interactions contributing to the relaxation pathway or both (evidence for a longer correlation time was reached from ^{13}C n.m.r. data). Comparison of R_i^s of

Table 7. ^1H-{^1H} N.O.e.s in 0.2 mol dm^{-3} solutions in [$^2H_6$]DMSO

Irradiated		Observed (1)	Observed (4)
O(1)H	N(1)H	0.027	
	C(1)H	0.115	0.151
C(1)H	N(1)H	0.049	0.023
C(3)H	N(1)H	0.058	0.068
	C(4)H	0.008	
N(1)H	C(1)H	0.063	0.186
	C(3)H	0.059	0.069
N(2)H	C(1)H	0.045	
	C(3)H	0.007	

Errors in the n.O.e.s were evaluated at ±10%.

the N(1)H proton yields the same evidence, once again demonstrating the pecularity of compound (**1**).

^1H-{^1H} *Nuclear Overhauser Enhancement Data.*—The origin of ^1H-{^1H} n.O.e.s has been extensively investigated.[11] The fractional n.O.e. of an observed spin *d* when spin *s* is saturated is given by equation (10)[11] where equation (11) applies.

$$f_d(s) = 0.5\rho_{ds}/R_d - 0.5 \sum_{n \neq d,s} \rho_{dn} f_n(s)/R_d \qquad (10)$$

$$R_d = \sum_{d \neq j} \rho_{dj} + \rho_d^* \qquad (11)$$

The term ρ_d^* represents the contribution from relaxation mechanisms other than the dipolar proton–proton interaction and can be usually neglected in cases where the dipolar interaction with nitrogen is not important.[11] Equation (10) holds under the assumption of negligible intermolecular dipolar interactions and for loosely coupled spin ½ systems.

Inspection of n.O.e. data, reported in Table 7, immediately shows that more proton–proton dipolar interactions can be measured in (**1**) than in (**4**) (in agreement with proton spin–lattice relaxation rate analysis). The two fC(1)H(N_2H) and fC(3)H(N_2H) n.O.e.s, measured in (**1**), are particularly relevant: the much larger value of the former n.O.e. indicates that the N(2) amide group is nearer to C(1)H than to C(3)H. These findings can only be explained by extensive bending of the side chain towards the ring.

It must be stressed that the relative distance is not the only parameter affecting the n.O.e. Cross-correlation and/or cross-saturation terms, as in equation (10), can make quantitative analysis a complicated matter,[11] especially in cases where the loose coupling approximation breaks down. In one case only is quantitative analysis feasible, namely when pre-saturation of two different protons, *s* and *m*, produces n.O.e. at the same proton *d*. Then from equation (10) relationship (12) can be drawn, provided cross-saturation terms are negligible.

$$\frac{f_d(s)}{f_d(m)} = \frac{r_{dm}^6}{r_{ds}^6} \qquad (12)$$

By applying equation (12) and the key distances obtained from proton spin–lattice relaxation rates [C(1)H–O(1)H 2.44 and 2.80 Å for (**1**) and (**4**), respectively], it was possible to calculate several interproton distances, as reported in Table 6.

The set of interproton distances in (**1**), coupled with consideration of the pecular chemical reactivity of this compound, can be accounted for by only one conformation, depicted in Figure 2 as a projection of the Dreiding model. This

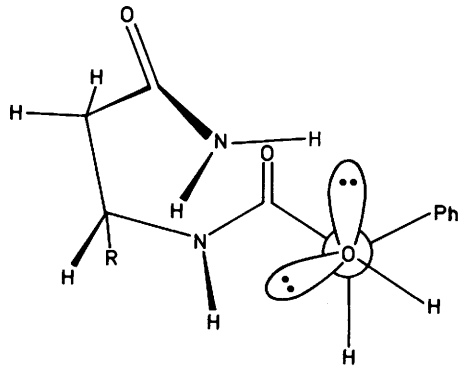

Figure 3. View of (**1**) showing involvement of the two lone pairs of the alcoholic oxygen in the hydrogen bonding network

conformation allows the possible formation of three intramolecular hydrogen bonds (i) between the carboxylic proton and the amide CO(NH) oxygen, (ii) between the NH proton and the alcoholic oxygen, and (iii) between the alcoholic oxygen and one of the protons of the amide NH_2 group. According to the literature for multicentre hydrogen bonds,[12] we may think of the last two as a bifurcated hydrogen bond (even if in a 'true' bifurcated hydrogen bond both hydrogens belong to the same atom).[12] These hydrogen bond pathways are shown in Figure 2. It is evident that these hydrogen bonds form a network of interactions which play a major and decisive role in stabilizing this conformation: the simultaneous presence of both kinds of hydrogen bonds provides the basis for different chemical behaviour as a result of the diverse preferred conformation in solution.

The conformation of (**1**) agrees with ^{13}C spin–lattice relaxation rates: a 'closed' structure is suitably related with severely restricted internal motions [if compared with 'open' structures as in (**3**) and (**4**)]; it also agrees with the *gauche* conformation of the CH(OH) fragment as calculated from ^1H spin–lattice relaxation rates: in one of the *gauche* conformers only the two lone pairs of the alcoholic oxygen are properly oriented for both hydrogen bonds (in the *anti* conformer one of the two lone pairs cannot at all be involved in intramolecular hydrogen bonds) (see Figure 3).

In (**1**) the lone pairs of the alcoholic oxygen are both engaged in hydrogen bonds and, at the same time, they are shielded by groups or hydrogen atoms brought around as a consequence of the particular conformation adopted. This being the situation it is quite hard for the reagent to approach them from whatever direction. In the other compounds only one of the two lone pairs could be engaged and, above all, the approach of the reagent is not hindered. This point is very likely to account for the surprising difference in chemical reactivity between (**1**) and the other molecules.

Similar considerations explain the chemical behaviour of the other diastereoisomer (**1a**) D-(−)-*N*-mandelyl-L-(−)-asparagine, and of the two corresponding mandelylaspartic acids.

Experimental

The studied compounds were prepared by the literature procedure cited: L-(+)-*N*-mandelyl-L-(−)-asparagine [N^2-L-(+)-(2-hydroxy-2-phenylacetyl)-L-(−)-asparagine] (**1a**), m.p. 158—159 °C;[2] *N*-mandelyl-2-amino-4-oxopentanoic acid {*N*-[2-(1-carboxy-3-oxo)butyl]-α-hydroxy-α-phenylacetamide} (**3**), m.p. 162—164 °C;[13] *N*-mandelyl-L-(−)-2-aminobutanoic acid {*N*-[2-(1-carboxy)propyl]-α-hydroxy-α-phenylacetamide} (**4**),

m.p. 111—113 °C.[2] Solutions were made in 99.8% [$^2H_6$]DMSO (Merck) and were carefully deoxygenated.

N.m.r. measurements were carried out with a Varian XL-200 Fourier Transform spectrometer. Chemical shifts were referred to internal tetramethylsilane. Spin–lattice relaxation rates were measured using the inversion recovery pulse sequence. Four and 100 f.i.d.s were collected for ^1H and ^{13}C T_1 measurements, respectively. The relaxation rate was calculated with a three-parameter exponential regression analysis of the recovery curves of longitudinal magnetization components. Selective and doubly selective relaxation rates were measured using inversion recovery pulse sequences where the 180° pulse was given by the proton decoupler at the selected frequencies at low power for relatively long times.[14] A typical setting for a selective 180° pulse was 20 db power attenuation and 20 ms pulse width. The selective rate was measured in the initial slope approximation[15] by considering the first part only of the recovery curve. ^{13}C-$\{^1H\}$ and ^1H-$\{^1H\}$ n.O.e.s were measured with gated decoupling techniques using n.O.e. difference pulse sequences.

References

1 G. Adembri, *Gazz. Chim. Ital.*, 1954, **84**, 1117.
2 G. Adembri and G. Bucci, *Ann. Chim.*, 1956, **46**, 69.
3 L. Hunter in 'Progress in Stereochemistry,' ed. W. Klyne, Butterworths, London, 1954, vol. 1, p. 223.
4 J. R. Lyerla, jr., and G. C. Levy, in 'Topics in Carbon-13 NMR Spectroscopy,' ed. G. C. Levy, Wiley, New York, 1974, vol. 1, p. 79.
5 F. W. Wehrli, in 'Topics in Carbon-13 NMR Spectroscopy,' ed. G. C. Levy, Wiley, New York, 1976, vol. 2, p. 343.
6 A. Allerhand, D. Doddrell, and R. Komoroski, *J. Chem. Phys.*, 1971, **55**, 189.
7 F. W. Wehrli and T. Wirthlin, 'Interpretation of Carbon-13 NMR Spectra,' Heyden, London, 1980.
8 C. W. M. Grant, L. D. Hall, and C. M. Preston, *J. Am. Chem. Soc.*, 1973, **95**, 7742.
9 L. D. Hall, *Chem. Soc. Rev.*, 1975, **4**, 401.
10 L. D. Hall, K. F. Wong, and H. D. W. Hill, *J. Chem. Soc., Chem. Commun.*, 1979, 951.
11 J. H. Noggle and R. E. Schirmer, 'The Nuclear Overhauser Effect,' Academic Press, New York, 1971.
12 R. Taylor, O. Kennard, and W. Versichel, *J. Am. Chem. Soc.*, 1984, **106**, 244.
13 D. Ben-Ishai, J. Altman, Z. Bernstein, and N. Peled, *Tetrahedron*, 1978, **34**, 467.
14 G. Valensin, G. Sabatini, and E. Tiezzi, in 'Advanced Magnetic Resonance Techniques in Systems of High Molecular Complexity,' eds. N. Nicccolai and G. Valensin, Birkhauser, Boston, 1986, p. 69.
15 R. Freeman, H. D. W. Hill, B. L. Tomlinson, and L. D. Hall, *J. Chem. Phys.*, 1974, **61**, 4466.

Received 1*st June* 1987; *Paper* 7/956